Electrical resistivity imaging data for hydrological and soil investigations of virgin Rospuda river peatland (North-East Poland).

Grzegorz Sinicyn[1], Łukasz Kaczmarek[1], Radosław Mieszkowski[2], Stanisław Mieszkowski[2], Bartosz Bednarz[1], Krzysztof Kochanek[1], Mateusz Grygoruk[3], Maria Grodzka-Łukaszewska[1]

[1]Faculty of Building Services, Hydro and Environmental Engineering, Warsaw University of Technology, Warsaw, 00-653, Poland
[2]Faculty of Geology, University of Warsaw, Warsaw, 02-089, Poland
[3]Institute of Environmental Engineering, Warsaw University of Life Sciences, Warsaw, 02-776, Poland

Correspondence to: Łukasz Kaczmarek (lukasz.kaczmarek@pw.edu.pl)

Abstract. The paper deals with the application of the method of geophysical for the investigation of the near-subsurface *fragile* hydrological environments. Study delivers ~~This publication presents~~ data ~~on~~ geophysical measurements data performed in the Rospuda wetlands located in North-Eastern Poland. The measurements were carried out by means of the the Electrical Resistivity Imaging (ERI; also called Electrical Resistivity Tomography, ERT) method, which so far was ~~to our best knowledge~~ never used in this region of the~~e~~ River Rospuda wetland valley. The ERI data were collected in single survey campaign in November 2022 to account for the wet season. During the campaign two ERI profiles were measured. The aim of the field works was to provide the material for illustration of the arrangement of geological layers creating the wetland. The data repository contains detailed ~~data~~ descriptions for each survey site. The study revealed a strong interaction between groundwater, characterized by a thick sandy aquifer, and surface water. In this system, surface present peat constitutes the dominant soil component within the contact zone between groundwater and surface water (with drainage river type). Variations in this relationship will have a direct impact on peat stability and associated hydrological processes. The water-saturated peat electrical resistivity zone (10-40 Ωm) have thickness ranging from a few to several meters at the maximum (the highest thickness of peats is present near the Rospuda River).

~~The ERI data from the selected survey sites can be used first of all to create the conceptual numerical model of groundwater and surface water interaction in this environmentally valuable area, which is to a certain extent a scientific *terra incognita*, but also for hydrological investigation of hydraulic conductivity and hydrodynamic field, identify geological structure, and characterize engineering properties of the organic soils.~~

1 ~~Background~~Introduction

Peatlands constitute unique areas of the interaction between soil, groundwater and surface water (Limpens et al., 2008). The organic soils, extremely valuable for the environmental, due to their accumulation properties (water, carbon dioxide, organic

matter; Kane et al., 2019; Word et al., 2022), high compressibility and variable water permeability depending on the tension level (Paniagua, Long & L'Heureux, 2021; Long et al., 2022), constitute a great challenge in planning their protection and potential development. Due to challenging availability and high variability of geological conditions, all the data considering wetlands become a very important input for further analyses, numerical calculations, and field and laboratory tests. Mostly because of the environmental uniqueness of this case study areas, the non-invasive method of electrical resistivity tomography imaging (ERI; which does not need heavy transportation to be moved), fits perfectly into the circumstances of achievable tests; (i.e. Slater and Reeve, 2002; Kowalczyk et al., 2017; Minasny et al., 2019; Pezdir et al., 2021). ERI is a geophysical method used to investigate subsurface structures by measuring electrical resistivity variations. In environmental studies, it helps monitor soil water content distribution, soil structure (i.e., high resistivity diversity of peats: compare results of Pezdir et al., 2021 and Kaczmarek et al., 2024) as well as permafrost dynamics, which are important for assessing climate change impacts. Thus, it is particularly valuable for detecting changes in permafrost thawing, carbon-rich soil degradation (especially peats), and hydrological processes influenced by rising temperatures.

The research is of reference nature for peatlands occurring in this part of Europe, also because of the research technique, which used which provide continuous identification of ground variability. The study considers electrical resistivity imaging results of the exemplary section of the Rospuda River Valley, which structure is original (no anthropogenic influence). The field study is located in the East-Central Europe, North-Eastern Poland (close to the border with Belarus) – Figure 1. The research is of reference nature for peat bogs occurring in this part of Europe, because of the scope of research and the research techniques used which additionally allowed for continuous identification of soil variability in the subsoil area.
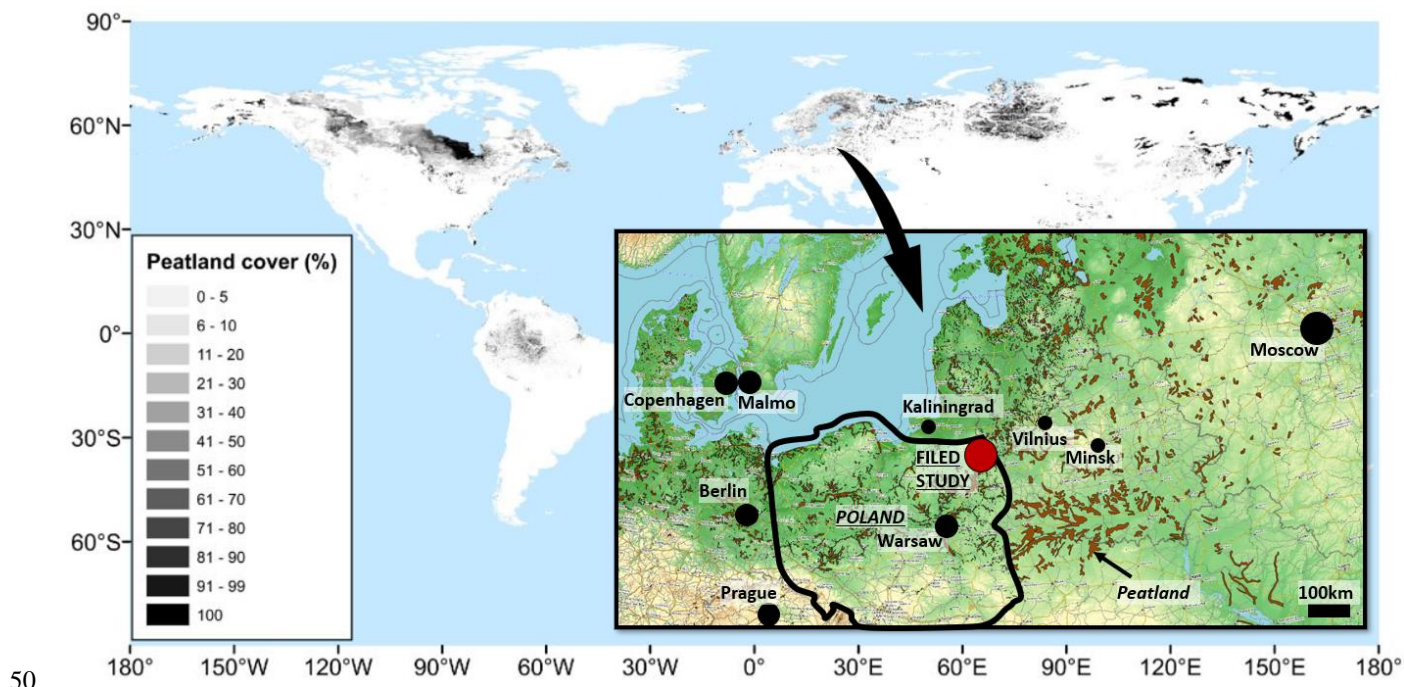
Figure 1: Localisation of the filed study at the background of the world peatland cover (modified Xu et al., 2017)

2 Material and methods

Rospuda River Valley was formed as the peatland, which developed in the large land depression in the Holocene (deglaciation of a Würm-Vistuilan Phase – Figure 2). The valley of the Rospuda River is vast (in the region of analysis, it ranges from around 0,5 km to 1,5 km), which is related to the glacial history of this region. Nowadays, the meandering river is in the middle (south part of the research area) and close to the west bank (north part of the research area) of the valley mentioned above, which has around 2,5 km between geophysical prospection lines. The analyzed area is surrounded by a large forest complex, where the entire region is a Rospuda Valley Protected Landscape Area (which partly constitutes also the Professor Aleksander Sokołowski Rospuda Valley Reserve). Figure 2 presents geomorphology with the topographic situation, the location of archival geological cross-sections (Figure 3), and the location performed within these study geophysical prospection lines.
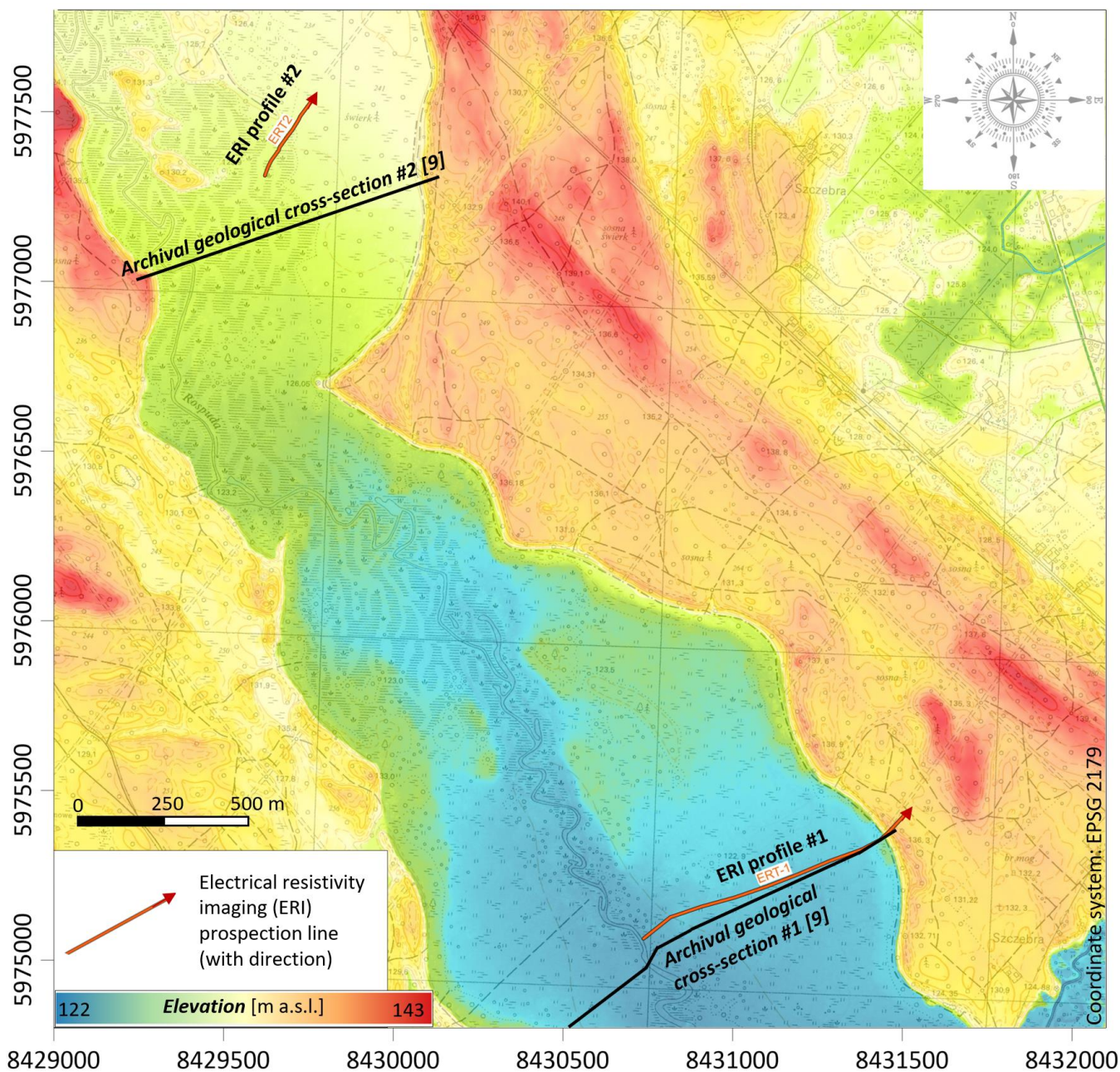
Figure 2: The ERI data distribution on the topographic map background (source: www.geoportal.gov.pl). Dark blue colour means the lowest elevation, where dark red the highest one).

This area is representative for many similar peatlands in northeastern Poland. Rospuda River Valley hosts one of the last large, well-preserved percolation mires (rich fen system) remaining in Central Europe (Jabłońska et al., 2011; Jabłońska et al., 2014;

Jabłońska et al., 2019). Figure 3 shows the geological structure (of the locations where the geophysical prospecting was done) in the form of cross-sections (Jabłońska et al., 2010 - below; Jabłońska et al., 2014 – schematic geological cross-section of the Rospuda valley along the riverbed described in the English) made on the basis of reconnaissance drilling.
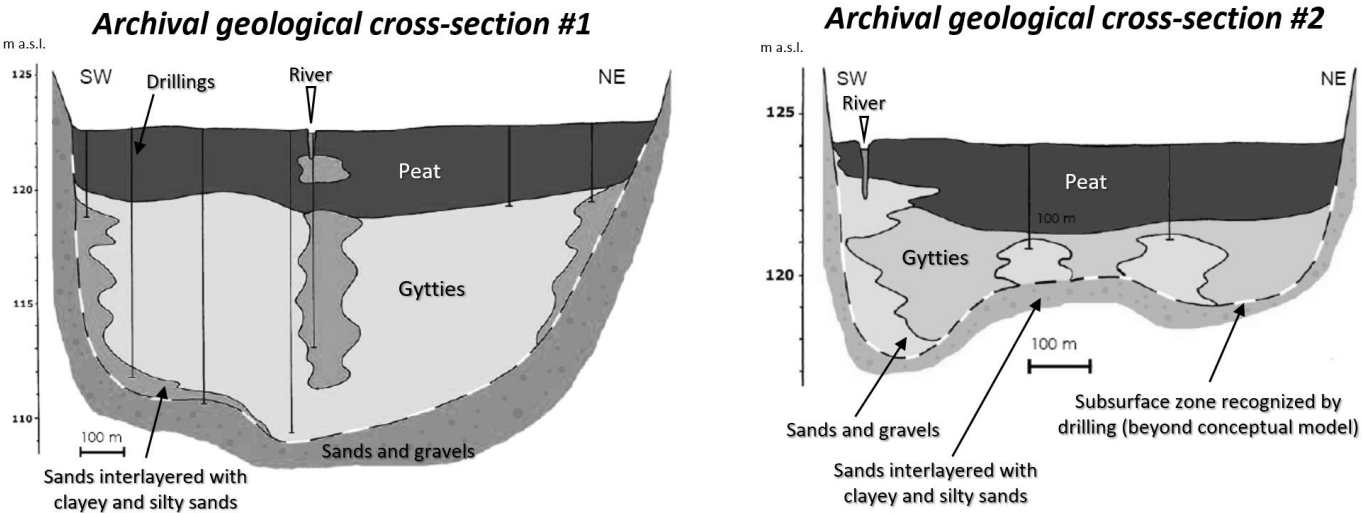
Figure 3: Archival geological cross-sections in the Rospuda research site (modified Jabłońska et al., 2010).

The two-dimensional resistivity imaging data were collected by galvanically injecting a low-frequency electrical current into the ground via two electrodes and measuring the voltage difference between two potential electrodes (detailed methodology aspects described in i.a. Loke, 2018). Differences in resistivity values caused by the flow of electric current through various subsurface mediums are used to identify materials (i.e. materials listed in Table 1). Electrical resistivity of the subsurface material is determined by the composition of soil (particle size distribution, mineralogy), its structure (porosity, pore size distribution, connectivity), fluid content, the concentration of dissolved electrolytes, the clay content, and the temperature (Palacky, 1988; Loke, 2018; Tarnawski, 2020). Table 3 depicts the electrical resistivity characteristics (inverse of conductivity) of common soil types (and water for comparison) in this area of Poland.

Table 1: Typical electrical resistivity of materials (based on Tarnawski, 2020 and authors' experience).

Selected materials	Typical range of electroresistivity (Ωm)
Clayey deposits (clay, till with clay)	<25
Organic soil (peat, alluvion)	10-100 (in aeration zone: 30-100; in saturation zone: 10-50)
Tills and loams	25-70
Sandy deposits	70-1000 (in aeration zone: 200-1000; in saturation zone: 90-250)

Surface water	0.1-300
Rainwater	30-1000
Mineralised water (i.a. sea water)	0.1-5
Permafrost	high

The advanced multi-electrode resistivity sensors were used to measure numerous data points in a single ERI profile by automatic switching of the current and potential electrodes. A multiple-gradient array was used to collect resistivity data in the both forward and backward survey directions. Figure 4 depicts the acquisition of field ERI data with the one of the most advanced 12-point light ABEM Terrameter LS-2 setup (Figure 4a). The electrodes were driven along the profiles and connected to cables with the cable joints for 21 take-out cables , which lead to a resistivity meter during resistivity measurements. The electrodes were tested for the contact resistance before each measurement session, and apparent resistivity was measured. Then, apparent resistivity in many of data points can be measured for a single ERI profile (eventually, giving the effect of *quasi* continues section). The multiple-gradient array was described in detail i.a. by Loke (2018).
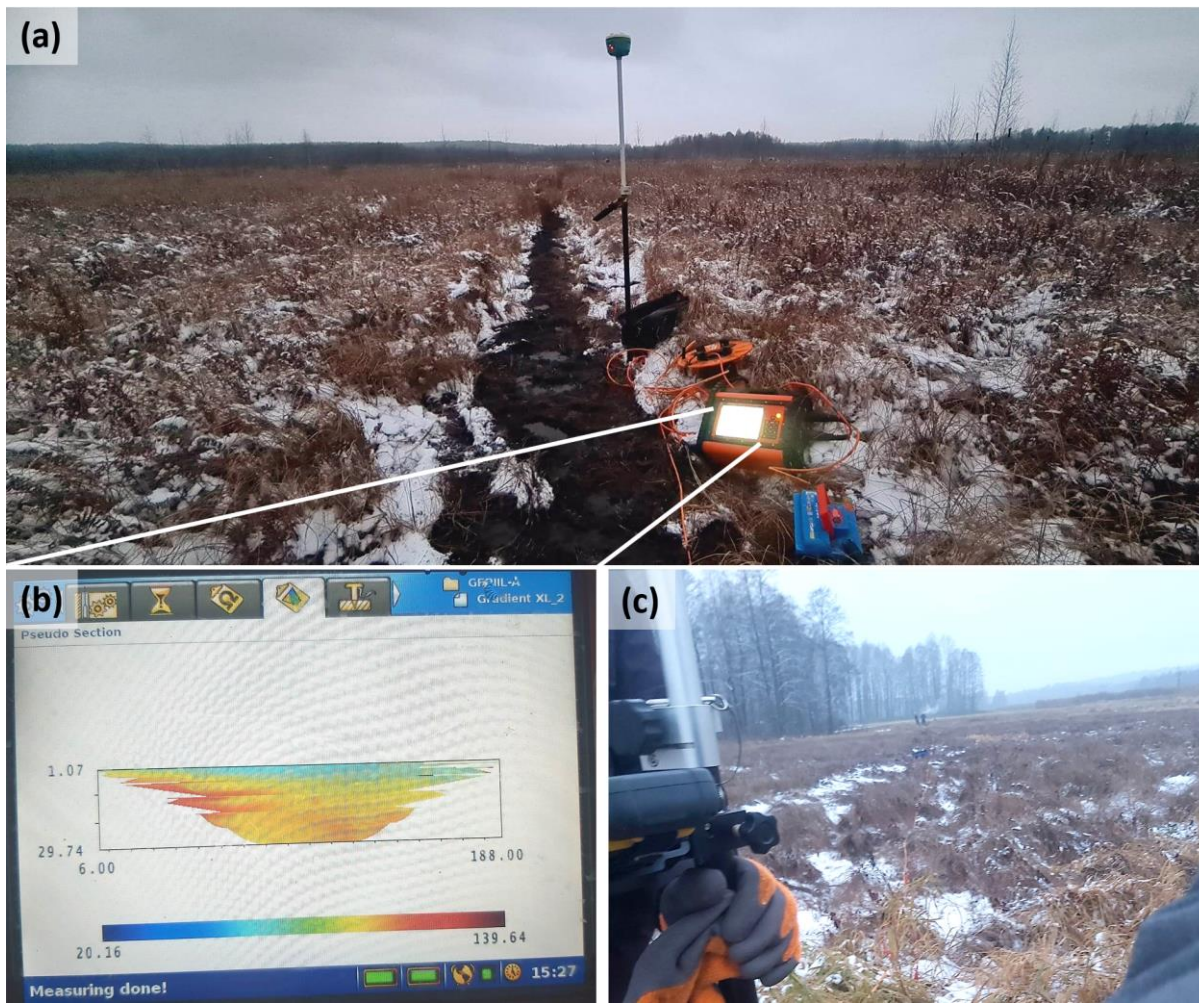
Figure 4: Acquiring ERI field data with multi-electrode (a) 12-point light Abem Terrameter LS-2 set-up at ERI profile No. 1, (b) raw visualization of results; (c) ERI profile No. 2.

The measured datasets were filtered to minimise noise. The RES2DINV software package (Aarhusgeosoftware Manual, 2022) was used for data processing and inversion. The smoothness-constrained least-square (DeGroot-Hedlin and Constable, 1990) and robust inversion (Wolke and Schwetlick, 1988) algorithms were used for data processing, depending on the expected subsurface features. However, the ERI data were mostly inverted by means of the smoothness-constrained least-square inversion algorithm. The iterative inversion method was applied until the discrepancy between measured and predicted resistivity data reached acceptable levels, i.e. when the root mean square (RMS) error dropped below 5% (information about the difference between the measured and calculated apparent resistivity values). This value may be exceeded for surveys in hard rock and noisy environments. As an example, we show the ERI data distribution (Figure 5) for resistivity data collected from the Rospuda site – prospection depth: ca. 32 m (profile #2) and 43 m (profile #1) b.t.s. These figures are important for

providing a sketch of the roll-along distribution of the acquired data. That will allow for the identification of any empty zones (areas without data, i.e. surface layer), density of data points (as well as number of related to them model blocks), and for verifying the final resistivity model.
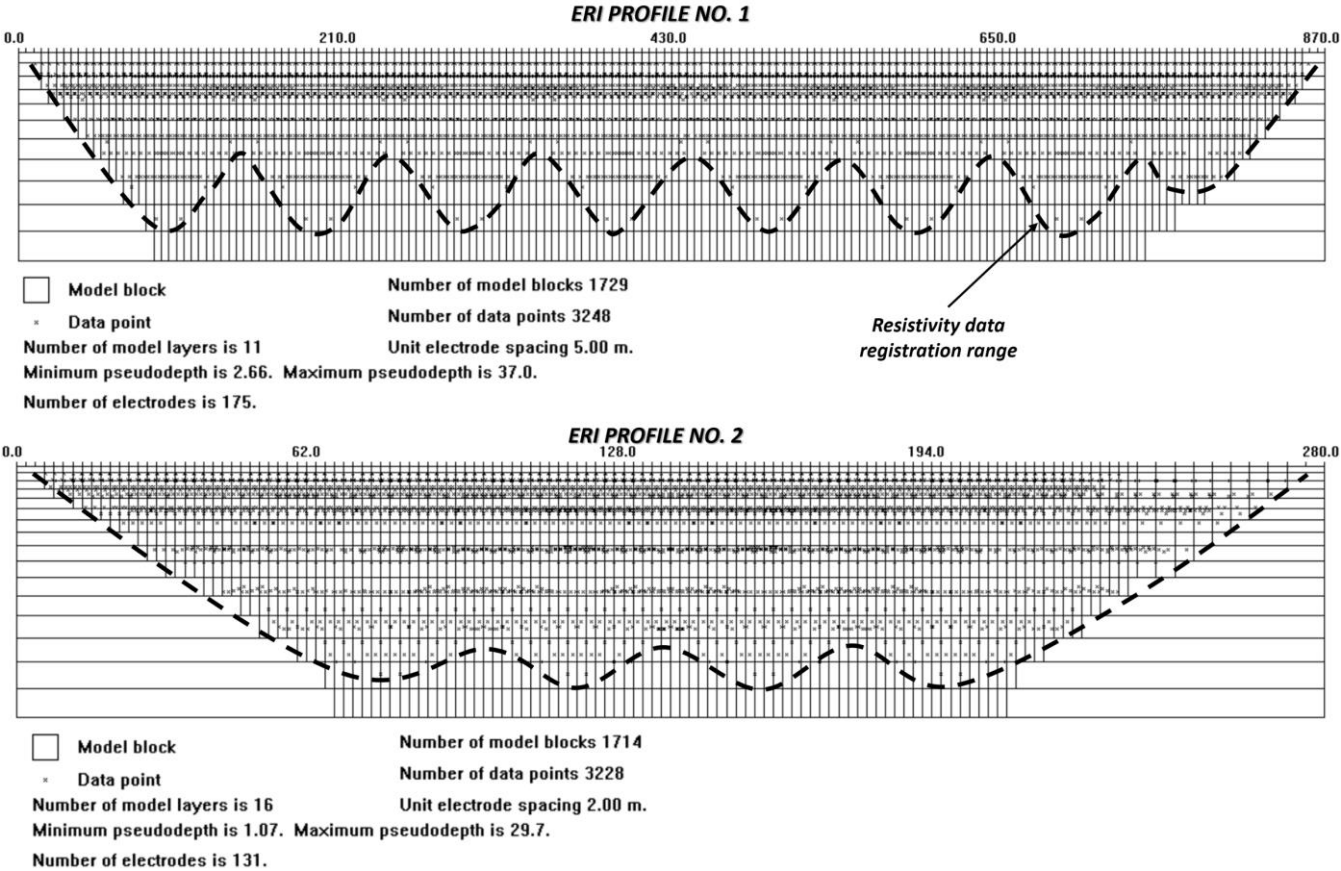
Figure 5: Electrical resistivity data points distribution and arrangement of model blocks: ERI profile No. 1 and 2 at the Rospuda site

The peatland developed in the large land depression in Holocene (deglaciation of a Würm-Vistuilan Phase) that forms Rospuda River Valley. This area is representative for many similar peatlands in northeastern Poland. Rospuda River Valley hosts one of the last large, well preserved percolation mires (rich fen system) remaining in Central Europe (Jabłońska et al, 2010; Jabłońska et al., 2011; Jabłońska et al., 2014; Jabłońska et al., 2019). Figure 1 shows the geological structure (of the locations where the geophysical prospecting was done) in the form of cross-sections (Jabłońska et al., 2010) made on the basis of reconnaissance drilling.

120
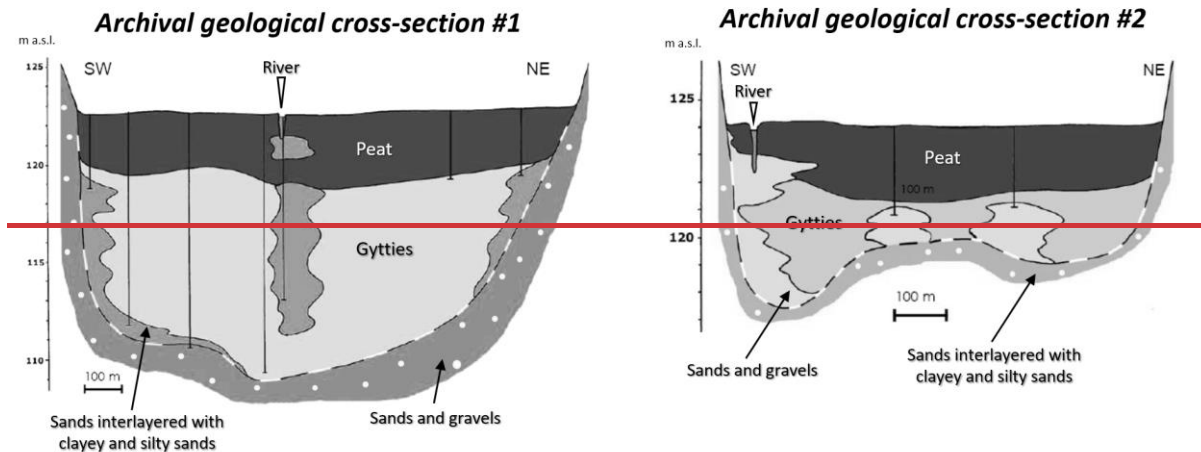
Figure 1: Archival geological cross-sections in the Rospuda research site (modified Jablońska et al., 2010).

125 **2 Results** ~~Data description~~

~~The data consider electrical resistivity imaging results for hydrological and geological investigations conducted in the reference~~ ~~Polish location (Figure 2).~~ The resulted ERI data of this important case study ~~They~~ can be easily accessible at Mendeley's data repository (Sinicyn et al., 2024): https://data.mendeley.com/datasets/5m34cs5zn4/4 ~~https://data.mendeley.com/datasets/10.17632/~~ 5m34cs5zn4/1. The

130 repository is structured into a folder - *ERI Rospuda Data*, which contains: raw data (presented general array format; in "dat" files) and inverted resistivity models images for each ERI profile (presented in "jpg" files). The Google Earth KML (Keyhole Markup Language) files with the location of the ERI profiles are also provided for each survey site. The data are of comparable ~~high~~ good quality because all the ERI profiles have been measured by the same ABEM Terrameter LS-2 setup by Multiple gradient array (~~r~~Roll-~~-a~~Along technique) with 5 m (profile #1) and 2 m (profile #2) electrode spacing. For the first ERI profile

135 performed using the roll-along technique, 7 stations (central unit positions - Terramter) were required. For the second, shorter ERI profile, 5 stations were necessary.

~~Below, Table 1, field photos, reference resistivity table, location map and selected exemplary results can be found.~~ Table 1 presents details on the ERI's metadata: profile line name, survey data, beginning and ending coordinates points of ERI profiles, elevation, profile orientation, array type, ~~electrode spacing,~~ profile length, filer type, file name, instrument info.

140 **Table 2** ~~1~~

ERI data resume descriptions for the Rospuda site.

Profile line name	Survey date (dd/mm/year)	ERI profile coordinates (X;Y in EPSG 2180)		Min and max elevation (m a.s.l. in PL-KRON86-NH)	Profile orientation	Profile length (m)	File name (and type)
		Begin	End				
1	26/11/2022	678040.9; 759131.6	678466.9; 759880.8;	122.5; 131.5	SW->NE	~~900~~ 870	ERI profile 1 (dat)
2	26/11/2022	680204.3; 757863.8	680452.3; 757997.5	124.4; 124.8	NW->SE	~~~280~~260	ERI profile 2 (dat)

Using the Roll Along technique, it was possible to obtain very valuable long prospecting lines (several hundred meters long). Figure 6 is about ERI profile No. 1: Figure 6a shows the distributions of apparent resistivity data, Figure 6b shows model calculated apparent resistivity data, and Figure 6c shows an inverted resistivity model. Figure 7 is about ERI profile No. 2. The images present electrical resistivity cross-sections with no rejected measurements (no such critical need; there were several that could be discussed but we wanted to show quality of "rough" data).
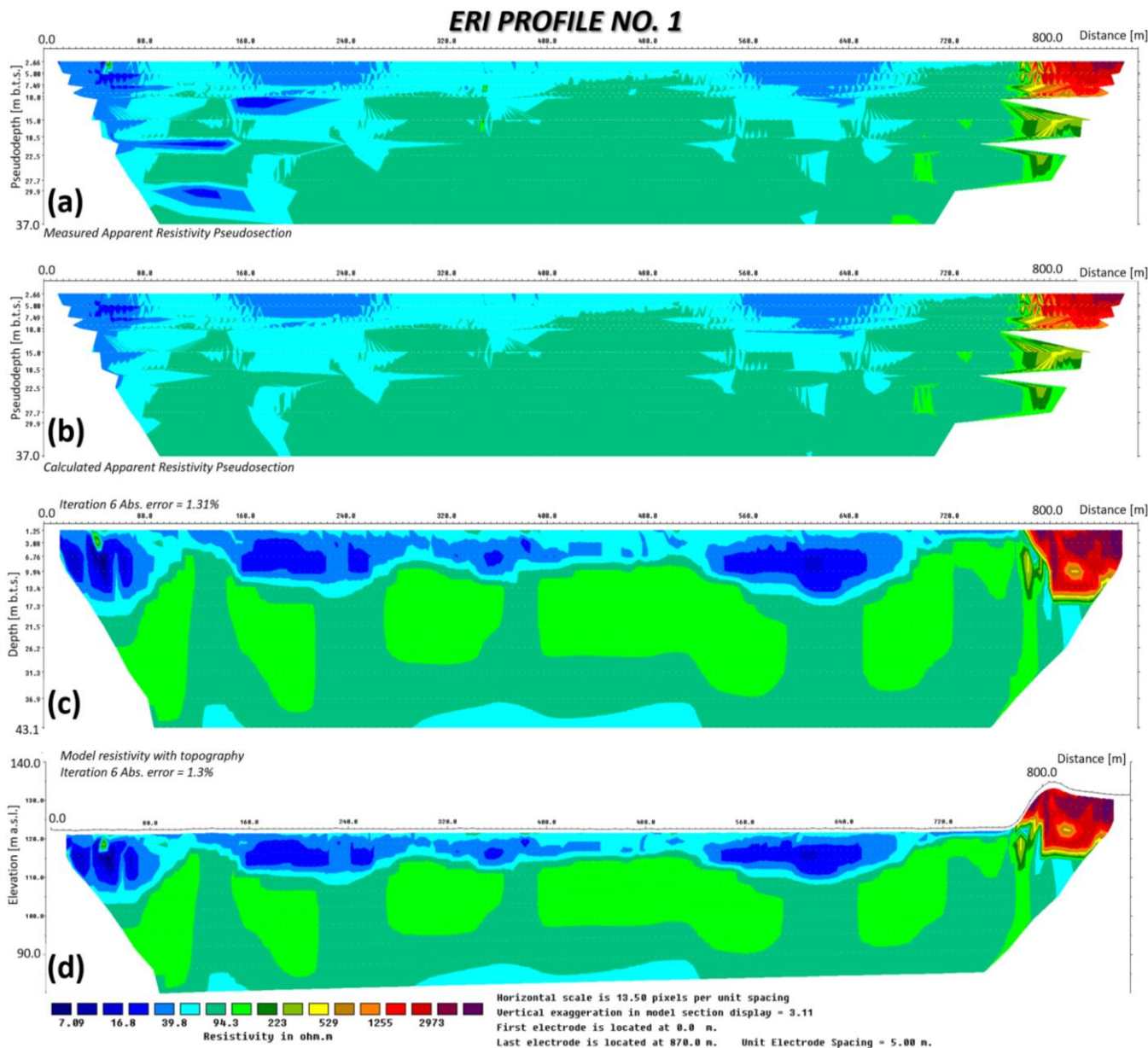
Figure 6: ERI profile No. 1 at the Rospuda site: (a) apparent resistivity data, (b) calculated apparent resistivity data, (c) inverted resistivity model, and (d) inverted resistivity model with topography.
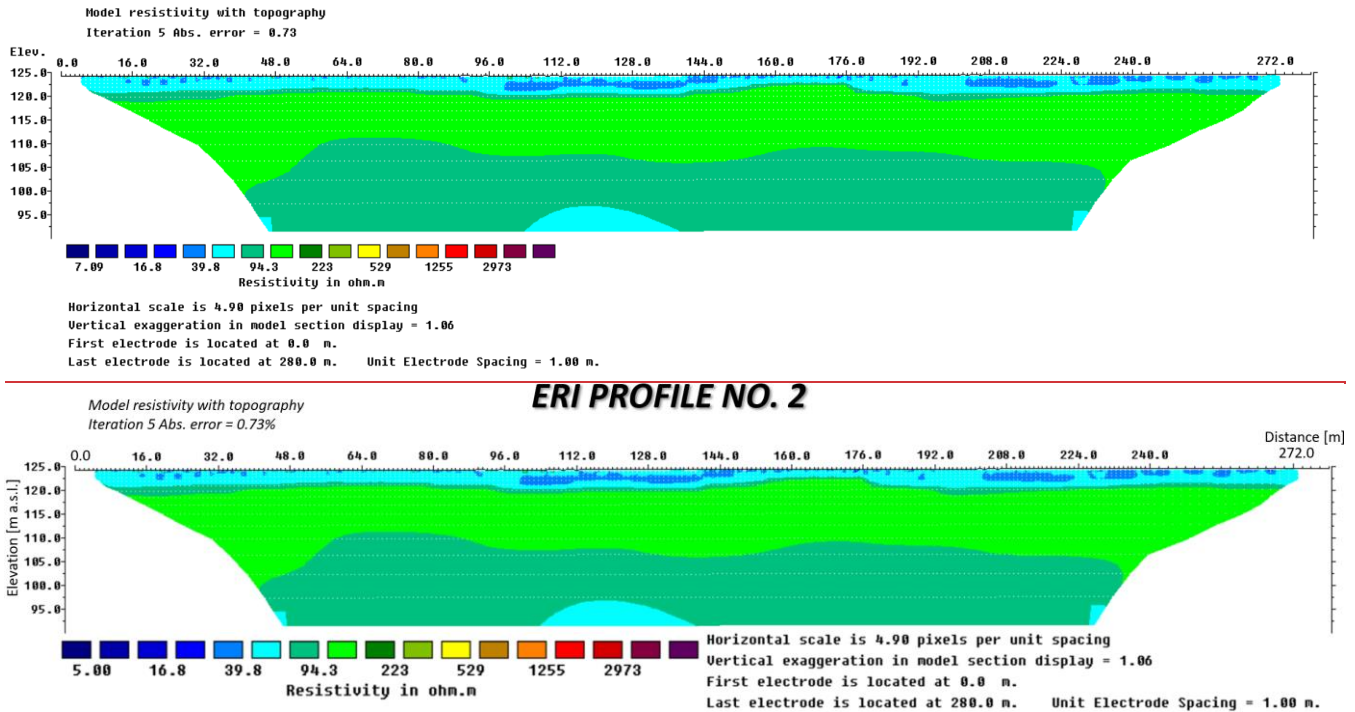
Figure 7: ERI profile No. 2 at the Rospuda site - inverted resistivity model with topography.

The obtained electrical resistivity images revealed the geological structure and the position of the water table very well. On the electrical resistivity cross-sections it is possible to distinguish: (i) a zone of very high resistivity, which corresponds to sands and gravels with very low water content constituting the high ground (a few thousand Ωm; maximum ~4310 Ωm); (ii) a zone of low resistivity (from ca. 75 Ωm to ca. 500 Ωm), occurring below the near-surface zone and which are most probably fully water saturated sands; (iii) a zone of even lower resistivity than Zone II (from ca. 40 Ωm to approx. 75 Ωm), which are water saturated silty sands (which may be overlain by clayey sands) - this zone is present at a relatively great depth of approx. 30 m; (iv) a zone of the lowest resistivity (10-40 Ωm), which is water-saturated peats of a thickness ranging from a few to several meters at the maximum (the highest thickness of peats is present near the Rospuda River). This interpretation corresponds to the geomorphology of the described area (detailed by Ber, 2007): the Rospuda River valley is a subglacial trough adjacent to sand plains in the west and east, within which numerous eskers and other forms of crevasses are present. This type of form was identified as an elevation in the first cross-section. The Rospuda River heads southeast, flowing approximately 2.5 km further into Lake Rospuda. Rospuda is a drainage river type, with groundwater recharge from the northwest and east. The groundwater table is in intense contact with the surface water of the Rospuda River. The influence of the water table level in the sand and gravel-type soils (Zone I) changes their electrical resistivity image (first cross-section),

causing a difference in resistivity of about 1000 Ωm (a decrease from about 4000 Ωm to about 3000 Ωm). This description indicates a thick Quaternary groundwater aquifer (no impermeable soil to a depth of about 43 m) with no more significant surface isolation layers in the form of soils like clays or tills. In this context, peats constitute a separate hydrogeological layer characterized by lower hydraulic conductivity than the surrounding mineral soils but with excellent retention properties.

175

Modifed Xu et al., 2017

3 Experimental design, materials and methods

The two-dimensional resistivity imaging data were collected by galvanically injecting a low-frequency electrical current into the ground via two electrodes and measuring the voltage difference between two potential electrodes (methodology based on Loke, 2018). Differences in resistivity values caused by the flow of electric current through various subsurface mediums are used to identify materials (i.e. materials listed in Table 3). Electrical resistivity of the subsurface material is determined by the composition of soil (particle size distribution, mineralogy), its structure (porosity, pore size distribution, connectivity), fluid content, the concentration of dissolved electrolytes, the clay content, and the temperature [Palacky, 1988; Loke, 2018; Tarnawski, 2020]. Table 3 depicts the electrical resistivity/conductivity characteristics of common subsurface geological materials in this area of Poland.

Table 3: Typical electrical properties of resistivity (inverse of conductivity) of common geological materials and other mediums in Poland (based on Tarnawski, 2020 and authors' experience).

Soil or other medium	Typical range of electroresistivity (Ωm)
Clayey deposits (clay, till with clay)	<25
Organic soil (peat, alluvion)	10-100 (in aeration zone: 30-100; in saturation zone: 10-50)
Tills and loams	25-70
Sandy deposits	70-1000 (in aeration zone: 200-1000; in saturation zone: 90-250)
Surface water	0.1-300
Rainwater	30-1000
Mineralised water (i.a. sea water)	0.1-5
Permafrost	high

The advanced multi-electrode resistivity sensors were used to measure numerous data points in a single ERI profile by automatic switching of the current and potential electrodes. A multiple-gradient array was used to collect resistivity data in the both forward and backward survey directions. Figure 3 depicts the acquisition of field ERI data with the one of the most advanced 12 point light ABEM Terrameter LS 2 setup (Figure 3a). The electrodes were hammered along the profiles and connected to cables with the cable joints for 21 take-out cables, which lead to a resistivity meter during resistivity measurements. The electrodes were tested for the contact resistance before each measurement session, and apparent resistivity was measured. Then, apparent resistivity in many of data points can be measured for a single ERI profile (eventually, giving the effect of *quasi* continues section). The multiple-gradient array was described in detail i.a. by Loke (2018).
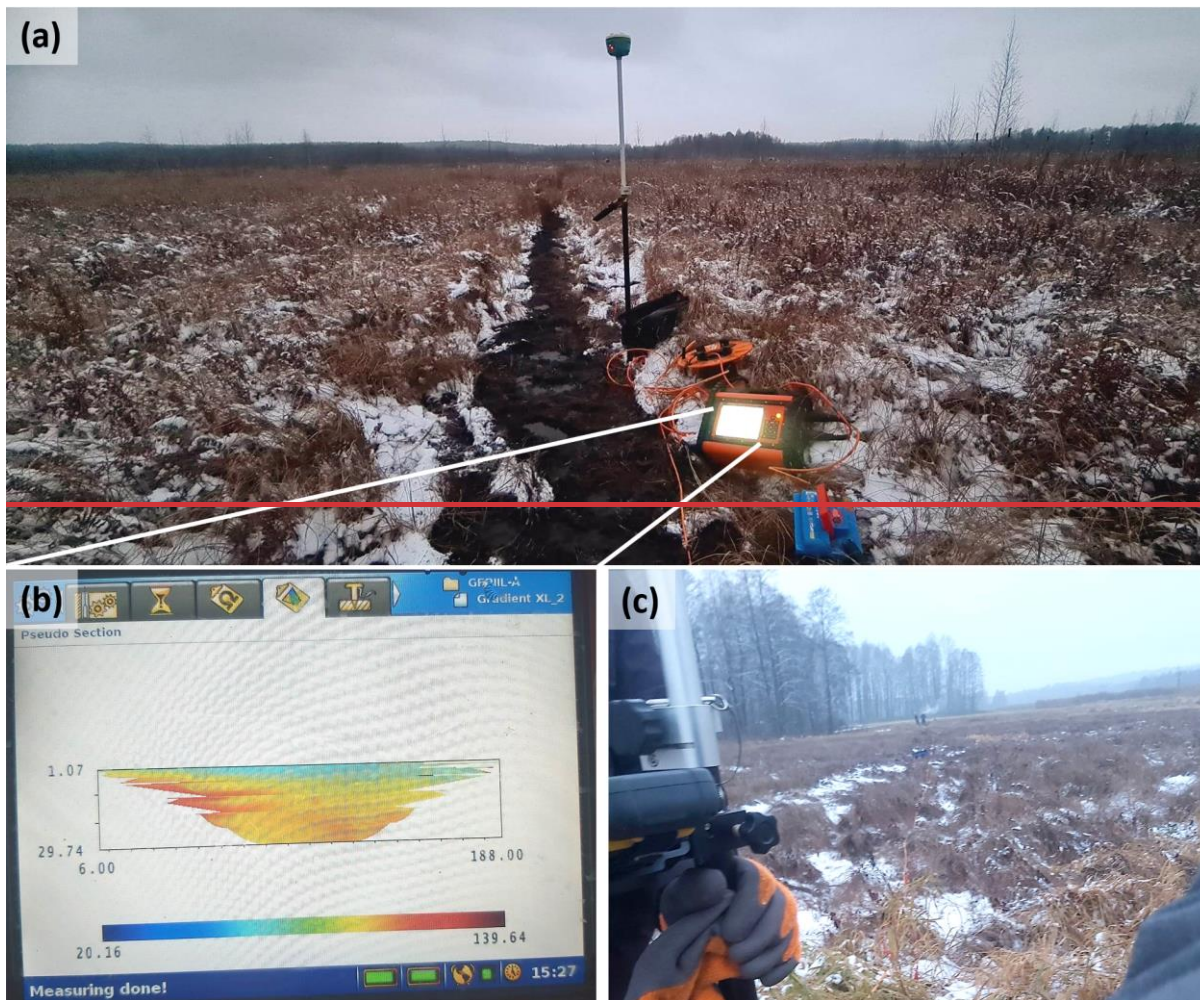
Figure 3: Acquiring ERI field data with multi-electrode (a) 12-point light Abem Terrameter LS-2 set-up at ERI profile No. 1, (b) raw visualization of results; (c) ERI profile No. 2.

The measured datasets were filtered to minimise noise. The RES2DINV software package (Aarhusgeosoftware Manual, 2022) was used for data processing and inversion. The smoothness-constrained least-square (DeGroot-Hedlin and Constable, 1990) and robust inversion (Wolke and Schwetlick, 1988) algorithms were used for data processing, depending on the expected subsurface features, however, the ERI data were mostly inverted by means of the smoothness-constrained least-square inversion algorithm. The iterative inversion method was applied until the discrepancy between measured and predicted resistivity data reached acceptable levels, i.e. when the root mean square (RMS) error dropped below 5% (information about the difference between the measured and calculated apparent resistivity values). This value may be exceeded for surveys in hard rock and noisy environments. As an example, we show the ERI data distribution (Figure 4) for resistivity data collected from the Rospuda site — prospection depth: ca. 32 m (profile #2) and 43 m (profile #1) b.t.s.

ARRANGEMENT OF MODEL BLOCKS AND APPARENT RESISTIVITY DATA POINTS

□ Model block
× Data point
Number of model layers is 11
Minimum pseudodepth is 2.66. Maximum pseudodepth is 37.0.
Number of electrodes is 175.

Number of model blocks 1729
Number of data points 3248
Unit electrode spacing 5.00 m.
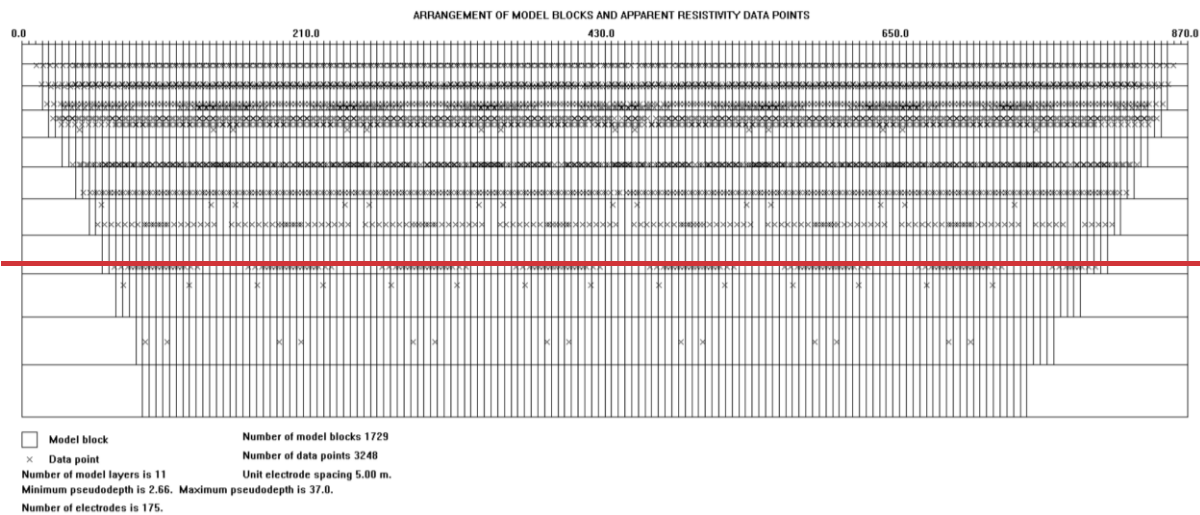
Figure 4: ERI profile No. 2 at the Rospuda site: the electrical resistivity data points distribution.

Using the Roll-Along technique, it was possible to obtain very valuable long prospecting lines (several hundred meters long). Figure 5a shows the distributions of apparent resistivity data, Figure 5b shows model calculated apparent resistivity data, and Figure 5c shows an inverted resistivity model.
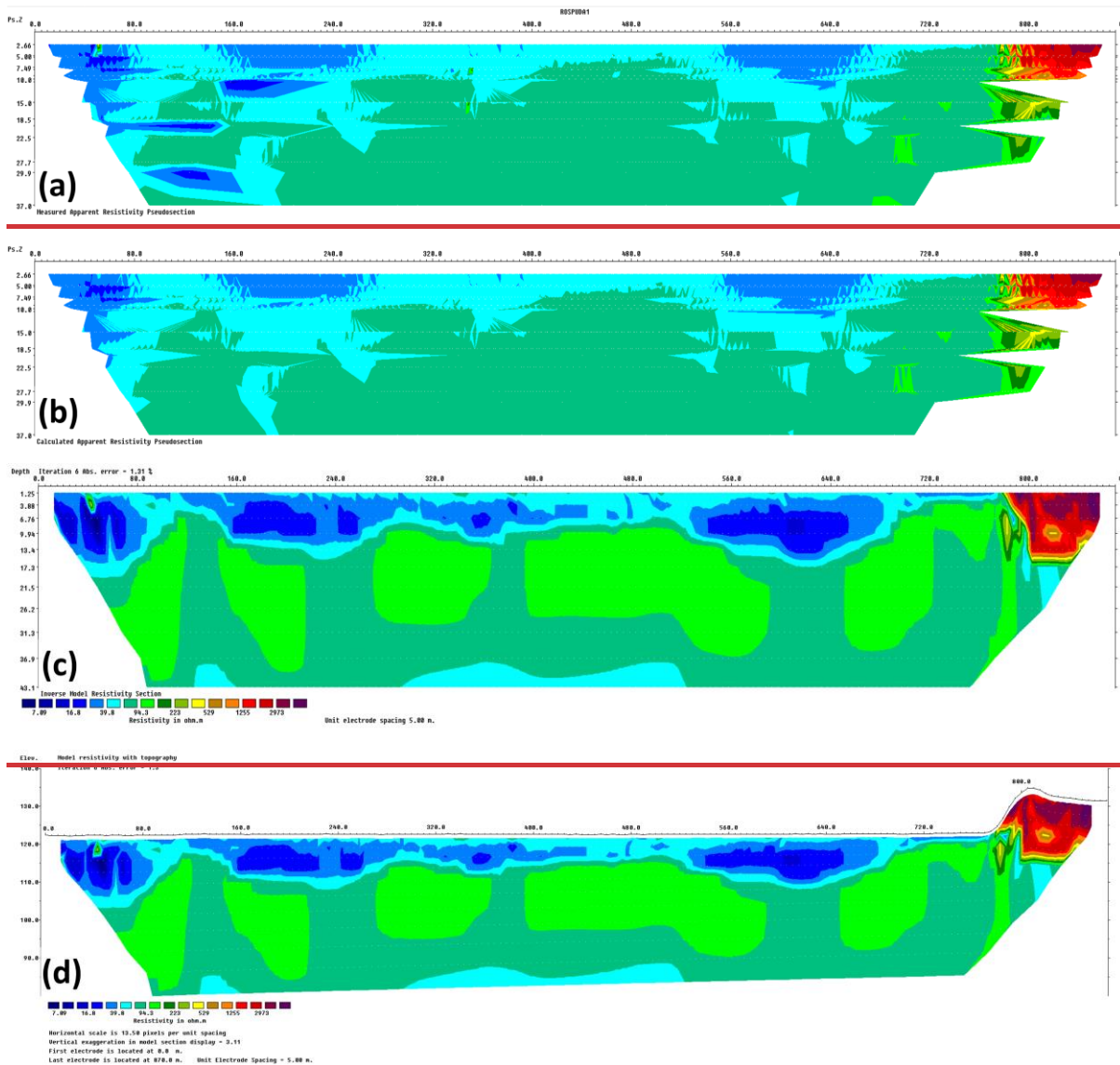
225 **4 Discussion**

4.1 Limitations

While conducting the research campaign by the ERI profiling we faced difficulties related to the high water saturation impact on the current field; in such a case the Terrameter revealed false data with zero or negative resistivity values, or quite contrary, large resistivity variation (especially near the surface). Such unexpected obstacles lead to the time-consuming results

230   processing or even made the measurements impossible. Fortunately during the investigation there was not rain and we manage to keep ERI set up not too much wet – thus we avoided the previously mentioned problems. Moreover, we managed to achieve a very low level of absolute error in iterations - in the first long profile this error was just 1.3% after six iterations and in the second case it was just 0.94% after 5 iterations.

4.2~~5~~ Data value

The Electrical Resistivity Imaging data from the selected survey site can be used to perform numerical modelling of groundwater and surface water interaction (i.e. van Loon et al., 2009; Grodzka-Łukaszewska et al., 2022) in the environmentally valuable area of the River Rospuda valley which is to a certain extend a scientific *terra incognita*, but also for hydrological investigations of hydraulic conductivity (related to lab/field tests, which can be even use for further resistivity conversion into a hydraulic conductivity value; Coe et al., 2018 Kaczmarek, Dąbska i Popielski, 2024, although these values should be regarded as indicative) and hydrodynamic field, identify geological structure, and characterize engineering properties of the organic soils. Determining a precise relationship between geophysical parameter values and the hydraulic conductivity is a complex challenge (Kirsch, 2009). Nevertheless, there are studies showing such (local) relation, i.e. $R = 8,14e^{1,23 \cdot k}$, where e is the exponential constant, R (Ωm) is the average resistivity of the aquifer, and k (m/d) is the hydraulic conductivity of the aquifer. (Lu, Huang & Xu, 2021).

The ERI data can be used to monitor groundwater heads (Chang et al., 2023) or generally hydrogeological conditions (i.e. Kowalczyk et al., 2014) as well as terrain changes (mainly subsidence due to water loss in the wetland's body) by comparing with future surveys. It can be related to the climate change effects.

The ERI data can be jointly inverted and interpreted with other field measurements (i.a. other geophysical methods, boreholes) to obtain more reliable subsurface information. Studies such as recognition drilling and probing (i.e. Carrière and Chalikakis, 2021), sampling and hydraulic conductivity lab tests (Kaczmarek et al., 2023), low-flow filed pumping tests, seismic, electromagnetic, and ground penetrating radar can be effectively integrated with ERI data.

Through open-source inversion algorithms, raw ERI data can be reprocessed to generate 2D and 3D inverted models (i.e. Cockett et al., 2015). Machine learning and statistical algorithms can be used to further interpretation of the inverted resistivity data.

5 Summary

The study investigates the application of Electrical Resistivity Imaging (ERI) to analyse the near-subsurface characteristics of a complex hydrogeological environment: the Rospuda River peatland in Poland. In recent years, interest in applications of the ERI method has increased, also in the context of peatland research and the assessment of climate change impacts on these fragile geological environments. The presented case study demonstrates the feasibility of ERI for detailed characterization of

soil lithological layers, including their geometry, as well as for identification of the water table. Despite challenging field conditions, including wet and winter weather, the acquired electrical resistivity data were of good quality. The study area, the Rospuda river valley, is a subglacial trough surrounded by eskers and located on an outwash plain. These geomorphological features play a crucial role in shaping local hydrogeological conditions. The study revealed a strong interaction between groundwater, characterized by a thick sandy aquifer, and surface water. In this system, surface present peat constitutes the dominant soil component within the contact zone between groundwater and surface water (with drainage river type). Variations in this relationship will have a direct impact on peat stability and associated hydrological processes.

Data availability

Datasets used in this article: Sinicyn, G., Mieszkowski, R., Kaczmarek, Ł., Mieszkowski, S., Bednarz , B., Kochanek, K., Grygoruk, M., Grodzka-Łukaszewska , M.: Electrical resistivity imaging data for hydrological and geological investigations of virgin Rospuda river peatland (North-East Poland) - original data, Mendeley Data, V2, doi: 10.17632/5m34cs5zn4.2, 2024.

Author contributions

SG: Conceptualization, Methodology, Data Collection, Writing- Reviewing and Editing. MR: Methodology, Data Collection, Data Processing. KŁ: Conceptualization, Methodology, Data Collection, Data Processing, Validation, Writing, and Original draft preparation. MS: Data Collection, Data Processing. BB: Data Collection, Writing- Reviewing and Editing. KK: Data Collection, Writing – Reviewing and Editing. MG: Writing – Reviewing and Editing, Funding Acquisition. G-ŁM: Conceptualization, Methodology, Data Collection, Writing, Original draft preparation.

Competing interests

The authors declare that they have no known competing financial interests or personal relationships that could have appeared to influence the work reported in this paper.

Acknowledgements

The research leading to these results has received funding from the Norwegian Financial Mechanism 2014-2021 (project no. 2019/34/H/ST10/00711).

References

Aarhusgeosoftware Manual for RES2DINVx64 ver. 4.10 with multi-core and 64-bit support. Aarhus, 2022.

Ber A.: Objaśnienia do szczegółowej mapy geologicznej Polski, w skali 1:50000, arkusz Augustów 147 (Explanations to the Detailed Geological Map of Poland, scale 1:50000, Augustów sheet 147). PIG-PIB, Warszawa, 2007.

Carrière, S. D., and Chalikakis, K.: Hydrogeophysical monitoring of intense rainfall infiltration in the karst critical zone: A unique electrical resistivity tomography data set, Data Brief, 40, 107762, doi: 10.1016/j.dib.2021.107762, 2021.

Chang, P. Y., Doyoro, Y. G., Lin, D. J., Puntu, J. M., Amania, H. H., and Kassie, L. N.: Electrical resistivity imaging data for hydrogeological and geological hazard investigations in Taiwan, Data Brief, 49, 109377, doi: 10.1016/j.dib.2023.109377, 2023.

Cockett, R., Kang, S., Heagy, L. J., Pidlisecky, A., and Oldenburg, D. W.: SimPEG: an open source framework for simulation and gradient based parameter estimation in geophysical applications, Comput. Geosci, 85, 142–154, doi: 10.1016/j.cageo.2015.09.015, 2015.

Coe, J. T., Brandenberg, S. J., Ahdi, S., and Kordaji, A.: *Geophysical methods for determining the geotechnical engineering properties of earth materials*. Temple University, 2018.

DeGroot-Hedlin, C., and Constable, S.: Occam's inversion to generate smooth, two-dimensional models from magnetotelluric data, Geophysics, 55, 1613-1624, doi: 10.1190/1.1442813, 1990.

Grodzka-Łukaszewska, M., Sinicyn, G., Grygoruk, M., Mirosław-Świątek, D., Kardel, I., and Okruszko, T.: The role of the river in the functioning of marginal fen: a case study from the Biebrza Wetlands, PeerJ, doi: 10.7717/peerj.13418, 2023.

Hulboj A., 2005. Objaśnienia do mapy hydrogeologicznej Polski pierwszy poziom wodonośny, skala 1:50000, arkusz Augustów 147 (Explanations to hydrogeological map of Poland first aquifer, scale 1:50000, sheet Augustów 147). PIG-PIB, Warszawa.

Jabłońska, E., Chormański, J., Falkowski, T., Jarzombkowski, F., Kłosowski, S., Okruszko, T., and Pawlikowski, P.: Hydrologiczno-hydrochemiczne uwarunkowania zróżnicowania przestrzennego roślinności i przebiegu procesów sukcesyjnych w ekosystemach torfowiskowych na przykładzie doliny Rospudy (Hydrological and hydrochemical determinants of spatial differentiation of vegetation and the course of succession processes in peatland ecosystems on the example of the Rospuda valley). University of Warsaw, Warsaw, 2010.

Limpens, J., Berendse, F., Blodau, C., Canadell, J. G., Freeman, C., Holden, J., Roulet, N., Rydin, H., and Schaepman-Strub, G.: Peatlands and the carbon cycle: from local processes to global implications – a synthesis, Biogeosciences, 5, 1475–1491, https://doi.org/10.5194/bg-5-1475-2008, 2008.

Jabłońska, E., Pawlikowski, P., Jarzombkowski, F., Chormański, J., Okruszko, T., and Kłosowski, S.: Importance of water level dynamics for vegetation patterns in a natural percolation mire (Rospuda fen, NE Poland), Hydrobiologia, 674, 105-117, doi: 10.1007/s10750-011-0735-z, 2011.

Jabłońska, E., Falkowski, T., Chormański, J., Jarzombkowski, F., Kłosowski, S., Okuszko, T., Pawlikowski, P., Theuerkauf,

320   M., Wassen, M., and Kotowski, W.: Understanding the Long Term Ecosystem Stability of a Fen Mire by Analyzing Subsurface
Geology, Eco-Hydrology and Nutrient Stoichiometry – Case Study of the Rospuda Valley (NE Poland), Wetlands, 34, 815-
828, doi: 10.1007/s13157-014-0544-z, 2014.

Jabłońska, E., Pawlikowski, P., Jarzombkowski, F., Tarapata, M., and Kłosowski, S.: Thirty years of vegetation dynamics in
the Rospuda fen (NE Poland), Mires and Peat, 24, 05, doi: 10.19189/MaP.2018.OMB.363, 2019.

325   Kaczmarek, Ł., Dąbska, A., and Popielski, P. Krótki przegląd badań współczynnika filtracji gruntów (Brief overview of soil
hydraulic conductivity testing methods). *Przegląd Geologiczny*, 70(5), 410–416, 2022.

Kaczmarek, Ł., Grodzka-Łukaszewska, M., Sinicyn, G., Grygoruk, M., Jastrzębska, M., and Szatyłowicz, J.: Hydraulic
Conductivity Tests in the Triaxial Stress State: Is Peat an Aquitard or an Aquifer? Water, 15(6), 1064, doi:
10.3390/w15061064, 2023.

330   Kane, E. S., Veverica, T. J., Tfaily, M. M., Lilleskov, E. A., Meingast, K. M., Kolka, R. K., and Chimmer R. A. Reduction-
oxidation potential and dissolved organic matter composition in northern peat soil: Interactive controls of water table position
and plant functional groups. Journal of Geophysical Research: Biogeosciences, 124, https://doi.org/10.1029/2019JG005339,
2019.

Kirsch, R.: *Groundwater geophysics* (2nd ed.). Springer. https://doi.org/10.1007/978-3-540-88405-7, 2009.

335   Kowalczyk, S., Zawrzykraj, P., and Mieszkowski, R.: Application of electrical resistivity tomography in assessing complex
soil conditions, Geological Quarterly, 59 (1), 367-372, doi: 10.7306/gq.1172, 2014.

Kowalczyk, S., Żukowska, K., Mendecki, M. J., and Łukasiak, D.: Application of electrical resistivity imaging (ERI) for the
assessment of peat properties: a case study of the Całowanie Fen, Central Poland, Acta Geophysica, 65, 223-235, doi:
10.1007/s11600-017-0018-9, 2017.

340   Loke, M. H. Tutorial: 2-D and 3-D electrical imaging surveys, Geotomosoft, Gelugor, 2018.

Long, M., Paniagua, P., Grimstad, G., Trafford, A., Degago, S., and L'Heureux, J.-S. *Engineering properties of Norwegian
peat for calculation of settlements*. *Engineering Geology*, 308, 106799. https://doi.org/10.1016/j.enggeo.2022.106799, 2022.

Lu, D., Huang, D., and Xu, C. Estimation of hydraulic conductivity by using pumping test data and electrical resistivity data
in fault zones. *Ecological Indicators, 129*, 107861. https://doi.org/10.1016/j.ecolind.2021.107861, 2021.

345   Minasny, B., Berglund, Ö., Connolly, J., Hedley, C., de Vries, F., Gimona, A., Kempen, B., Kidd, D., Lilja, H., Malone, B.,
McBratney, A., Roudier, P., O'Rourke, S., Rudiyanto, Padarian, J., Poggio, L., ten Caten, A., Thompson, D., Tuve, C., and
Widyatmanti, W. Digital mapping of peatlands – A critical review. *Earth-Science Reviews*, *196*, 102870.
https://doi.org/10.1016/j.earscirev.2019.05.014, 2019.

Palacky, G.: Resistivity characteristics of geologic targets: Electromagnetic methods in applied geophysics 1, 52-129, 1988.

350   Pezdir, V., Čeru, T., Horn, B., and Gosar, M. Investigating peatland stratigraphy and development of the Šijec bog (Slovenia)
using near-surface geophysical methods. *Catena*, *206*, 105484. https://doi.org/10.1016/j.catena.2021.105484, 2021.

Sinicyn, G., Mieszkowski, R., Kaczmarek, Ł., Mieszkowski, S., Bednarz, B., Kochanek, K., Grygoruk, M, and Grodzka-Łukaszewska, M.: Electrical resistivity imaging data for hydrological and soil investigations of virgin Rospuda river peatland (North-East Poland) - original data.Electrical resistivity imaging data for hydrological and geological investigations of virgin Rospuda river peatland (North-East Poland) - original data, Mendeley Data, ~~V1,~~ doi: 10.17632/5m34cs5zn4.410.17632/5m34cs5zn4.2, 2024.

Slater, L. and Reeve, A. Investigating peatland stratigraphy and hydrogeology using integrated electrical geophysics. *Geophysics*, 67(2), 365–378. https://doi.org/10.1190/1.1468597, 2002.

Paniagua, P., Long, M., L'Heureux, J-S. Geotechnical characterization of Norwegian peat: database. IOP Conf. Ser.: Earth Environ. Sci. 710, 012016, 2021.

Tarnawski, M. (ed.): Investigation of the ground of structures. Field methods, PWN, Warsaw, p.670, 2020.

Wolke, R., and Schwetlick, H.: Iteratively reweighted least squares: algorithms, convergence analysis, and numerical comparisons, SIAM J. Sci. Stat. Comput., 9, 907-921. http://doi.org/10.1137/09090, 1988.

van Loon, A., Schot, P., Griffioen, J., Bierkens, M., Batelaan, O., and Wassen, M.: Throughflow as a determining factor for habitat contiguity in a near-natural fen, Journal of Hydrology, 379 (1-2), 30-40, doi: 10.1016/j.jhydrol.2009.09.041, 2009.

Word, C. S., McLaughlin, D. L., Strahm, B. D., Stewart, R. D., Varner, J. M., Wurster, F. C., Amestoy, T. J., and Link, N. T. Peatland drainage alters soil structure and water retention properties: Implications for ecosystem function and management. Hydrological Processes, 36(3), e14533. https://doi.org/10.1002/hyp.14533, 2022.

Xu, J., Morris, P. J., Liu, J., Holden, J. PEATMAP: Refining estimates of global peatland distribution based on a meta-analysis. University of Leeds. [Dataset] https://doi.org/10.5518/252, 2017.